ACS OMEGA

http://pubs.acs.org/journal/acsodf

Article



# Royal Jelly Induces Thin Hair Shaft Formation by Suppressing Proliferation of Hair Follicle Stem Cells in Mice

Takumi Hamanishi, Haruta Koga, Takanori Nishimura, and Ken Kobayashi*

Cite This: *ACS Omega* 2025, 10, 17228−17236

Read Online

ACCESS | Metrics & More | Article Recommendations | Supporting Information

**ABSTRACT:** Royal jelly (RJ), a honeybee product, is used as a cosmetic and food ingredient to improve skin condition. However, the influences of RJ on hair growth remain unclear. In this study, we investigated whether RJ regulates hair follicle development, hair shaft formation, and proliferation of hair follicle stem cells (HFSCs) using a gentle anagen induction model by shaving the back skin and a forced anagen induction model by depilating the back skin in mice. The results showed that topical application of RJ on depilated skin induced thinning of the hair shaft and smaller hair bulb formation during the anagen phase. In addition, RJ suppressed the proliferation of CK15-positive HFSCs in hair follicles at the early and middle anagen stages of shaved back skin. RJ suppressed the proliferation of cultured HFSCs *in vitro*. These findings suggested that RJ induces the formation of thin hair shafts by suppressing the HFSC proliferation.

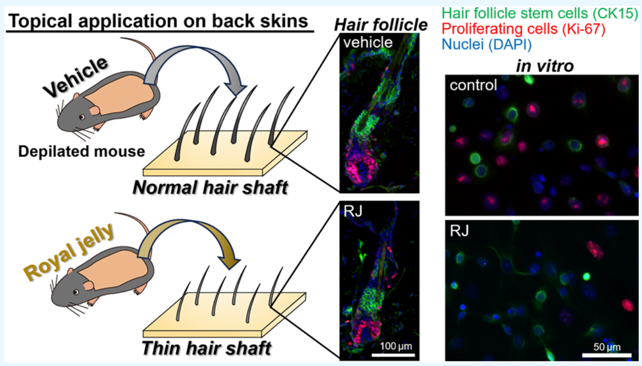


## 1. INTRODUCTION

Royal jelly (RJ) is a milky-white substance produced by nurse honeybees and is the primary food for queen bees. It contains water, sugars, proteins, lipids, and other minor components.[1] The protein and lipid fractions contain RJ-specific components such as royalisin, 10-hydroxydecanoic acid (10HDAA), and 10-hydroxy-trans-2-decenoic acid (10H2DA).[2] RJ and these components have multiple physiological activities such as antitumor, antioxidant, anti-inflammatory, and estrogen-like effects.[3] RJ is also known to facilitate wound healing by stimulating epidermal keratinocytes.[4] Hair follicles are skin appendages that form hair shafts and consist of keratinocytes that differentiate from hair follicle stem cells (HFSCs). Previously, we reported that propolis from a honeybee hive product stimulates hair growth in mice by activating keratinocyte proliferation. However, it remains unclear whether the RJ influences hair follicle development and shaft formation.

Hair follicles continuously cycle through anagen (growth), catagen (involution), and telogen (resting) stages.[5] In telogen hair follicles, HFSCs in a nonproliferating state reside in the bulge region of the outer root sheath of hair follicle and secondary hair germs at the lower end of the hair follicle.[6,7] After anagen phase induction, HFSCs actively proliferate and differentiate into progenitor cells. HFSCs and progenitor cells invaginate into the subcutaneous fat layer and differentiate into specific cells that make up each part of the hair follicle, such as the outer root sheath and hair bulbs, during the early and middle anagen phases. In the middle and late anagen stages, hair matrix cells in the hair bulbs actively proliferate and keratinize to form hair shafts, which grow and protrude from the skin. In the catagen stage, hair matrix keratinocytes stop proliferating and the structure of the hair follicle (hair bulb and outer root sheath) gradually regresses. Finally, the regressed hair follicles enter the telogen stage, and hair follicles and HFSCs are maintained in a quiescent state until anagen induction occurs. Thus, HFSCs play an essential role in hair follicle development and shaft formation during the anagen phase.

RJ and its components have been reported to activate or inactivate various signaling pathways, including the MAPK and Akt pathways.[8,9] Activation of MAPK and Akt signaling induces HFSC proliferation in the bulging regions of human hair follicles.[10] In addition, ERK/MAPK signaling is involved in the cytoprotective function of HFSCs and their hair-inducing capacity in mouse skin.[11] Akt signaling pathways are essential for *de novo* hair follicle regeneration and maintenance of HFSCs pool balance.[12] HFSC proliferation is activated via the PI3K/Akt pathway, whereas HFSC depletion is driven by p38/MAPK-induced cell death.[13] These reports suggest that RJ influences HFSCs by modulating activation of the Akt and

**Received:** October 7, 2024
**Revised:** April 7, 2025
**Accepted:** April 16, 2025
**Published:** April 22, 2025

MAPK pathways. However, the effect of the RJ on HFSCs remains unclear.

RJ has multiple physiological functions and facilitates wound healing. However, the effects of RJ on the skin appendages containing hair follicles remain unclear. In this study, we investigated whether RJ influenced hair follicle development, hair shaft formation, and HFSC proliferation in two *in vivo* mouse models. One is the gentle anagen induction model, which is prepared by shaving the back skin during the telogen phase to estimate the anagen induction ability of RJ treatment.[14] The second is the forced anagen induction model, which involves depilating the back skin during the telogen phase and immediately inducing synchronized entry into the anagen phase to evaluate the development of the hair follicle structure and hair shaft formation.[5,15] We prepared a culture model of skin epithelial cells containing HFSCs to investigate the effects of the RJ on HFSC proliferation. These experiments enabled us to reveal the potential of RJ to induce the formation of thin hair shafts by suppressing the HFSC proliferation.

## 2. MATERIALS AND METHODS

**2.1. Animals.** Seven-week-old female C57BL/6N mice were purchased from Japan SLC (Shizuoka, Japan). The mice were maintained under conventional conditions at 22−25 °C and given food and water ad libitum. After 1 week of acclimatization, the mice were subjected to forced anagen induction experiments by depilation of the back skin and gentle anagen induction experiments by shaving the back skin. Pregnant C57BL/6N mice were also purchased, and the 3-week-old pups were used for cell culture experiments. All experiments were approved by the Animal Resource Committee of Hokkaido University (permission number:18−0154) and performed in accordance with the Hokkaido University guidelines for the care and use of laboratory animals.

**2.2. Preparation of RJ.** Protease-treated RJ powder, which degrades RJ proteins into peptides and amino acids using proteases to reduce immunoreactivity and allergenicity without nutritional loss of minerals, vitamins, and fatty acids,[16] was obtained from Yamada Bee Company, Inc. (lot no. YRP-M-211213−2, Okayama, Japan). Protease-treated royal jelly contains 4.3% 10H2DA, 1.3% 10HDAA, 0.44% (*E*)-2-decenedioic acid, 0.36% (*R*)-3,10-dihydroxydecanoic acid, 0.31% 8-hydroxyoctanoic acid, 0.28% sebacic acid, 0.05% 12-hydroxydodecanoic acid, and 0.023% acetylcholine, as previously reported.[17] Protease-treated RJ was standardized to include a minimum of 3.5% 10H2DA and a minimum of 0.6% 10HDAA. For preparation of the RJ solution using topical application on mouse skin, protease-treated RJ powder was added to Dulbecco's (D)-PBS to a concentration of 20% and stirred at 4 °C for 16 h. After stirring, the mixture was centrifuged at 12,000*g* for 10 min at 20 °C. The supernatant was diluted 5-fold with water and mixed with an equal volume of ethanol. For preparation of the RJ solution using cell culture experiments, protease-treated RJ powder was added to DMEM/F-12 medium to a concentration of 1% and stirred at 4 °C for 16 h. After stirring, the solution was centrifuged, the supernatant was sterilized by filtration through a 0.22-$\mu$m-pore-size filter.

**2.3. Shaving and Depilation of Mice.** Shaving and depilation of the mouse back skin for gentle and forced anagen induction were performed as previously reported.[14] In brief, hair on the back skin of anesthetized mice was shaved using an electric shaver, and the hair cycle of the back skin was at the telogen stage was judged by skin color.[5] In the gentle anagen induction experiments, the 2% RJ solution was topically applied to the shaved skin at 100 $\mu$L/day after 1 week of shaving until hair shaft is observed on the caudal side of the back skin. D-PBS containing 50% ethanol was used as the vehicle control. In the forced anagen induction experiments, the back hair of anesthetized mice was shortened with an electric shaver and club hair was removed from the back skin using depilatory wax. One day after depilation, the 2% RJ solution was topically applied to the back skin at 100 $\mu$L/day for 12 d. D-PBS containing 50% ethanol was used as the vehicle control. The treated skin regions were excised and fixed in 4% formaldehyde in D-PBS for immunostaining of the whole skin and the preparation of paraffin sections. The excised skin was fixed in 2.5% glutaraldehyde (Taab Laboratories Equipment, Aldermaston, U.K.) in D-PBS for the observation of hair shafts on the skin surface by using a scanning electron microscope.

**2.4. Identification of Anagen Induction in Shaved Mice.** In shaved mice, the hair cycle progresses from the caudal end toward the cranial end of the back skin, and melanin granules are produced in the bulbs of middle anagen hair follicles.[18] In addition, hair shafts were observed on the skin surface after reaching the late anagen stage. Therefore, the middle and late anagen phases were visually identified based on melanization and hair shafts on the shaved back skin, respectively.

**2.5. Antibodies.** The following antibodies were used as primary antibodies for immunofluorescence staining and Western blotting: mouse antibodies against cytokeratin 15 (CK15; Thermo Scientific, Fremont, CA; #MS-1068P1), phosphorylated-NF$\kappa$B (pNF$\kappa$B; Cell Signaling Technology, Danvers, MA; #13346), myeloperoxidase (Santa Cruz Biotechnology, Dallas, TX; #sc-365436), rabbit antibodies against phosphorylated-Akt (pAkt; Cell Signaling Technology, #4060), Akt (Cell Signaling Technology; #4691), pERK (Cell Signaling Technology; #4370), ERK (Cell Signaling Technology; #4695), pp38 (Cell Signaling Technology; #4511), p38 (Cell Signaling Technology; #8690), a rat antibody against $K_i$-67 (DakoCytomation, Glostrup, Denmark; #M7249). Alexa Fluor-conjugated secondary antibodies for immunostaining were purchased from Thermo Fisher Scientific. Horseradish peroxidase-conjugated secondary antibodies for Western blotting were purchased from Sigma-Aldrich (St. Louis, MO).

**2.6. Immunofluorescence Staining.** The excised back skins were fixed with 4% formaldehyde in D-PBS and were embedded in paraffin for the preparation of paraffin sections sliced into 5-$\mu$m. The deparaffinized sections were heated in a microwave in antigen retrieval buffer consisting of 10 mM Tris−HCl (pH 9.0) and 0.5 mM ethylene glycol tetraacetic acid for 20 min (Sigma-Aldrich). The cultured cells were fixed with methanol at −20 °C for 10 min and then in 1% formaldehyde in D-PBS at 4 °C for 10 min, followed by permeable treatment with 0.2% Triton X-100 in D-PBS at room temperature for 10 min.

Samples were incubated with 5% bovine serum albumin (BSA) in D-PBS containing 0.05% Tween 20 (T-PBS) to block nonspecific interactions. The samples were then incubated for 2 days at 4 °C in primary antibodies diluted in 2.5% BSA in D-PBS. After the samples were washed with T-PBS for 40 min, they were exposed to secondary antibodies


https://doi.org/10.1021/acsomega.4c09123
ACS Omega 2025, 10, 17228−17236

diluted in the blocking solution for 1 h at room temperature. Negative controls were treated in the same manner but without primary antibodies. Images of the stained samples were acquired by using a fluorescence microscope (BZ-X810; KEYENCE, Osaka, Japan).

In the case of the whole-mount immunostaining of the skin, the skin was fixed with D-PBS containing 4% formaldehyde and shaken for 30 min at room temperature. The fixed skin was immersed in HEPES buffer containing 1% Triton X-100 and 5 mM $CaCl_2$ and shaken thrice for 10 min each. The skin was incubated overnight at 4 °C in the blocking solution (HEPES buffer containing 1% BSA and 5 mM $CaCl_2$) for 12 h followed by incubation for 7 days at 4 °C in primary antibodies diluted in the blocking solution. After the skin was washed with HEPES buffer containing 0.05% Tween-20 and 5 mM $CaCl_2$ for 12 h, they were exposed to secondary antibodies diluted in the blocking solution for 7 days at 4 °C. After washing for 24 h, the skin was immersed in Fluoromount G (Southern Biotech, Birmingham, AL) and crimped between two cover glasses. Fluorescent images of the stained skin samples were obtained using a confocal laser-scanning microscope (TCS SP5; Leica, Mannheim, Germany). The diameter of the hair bulb, indicated by the localization of CK15 and $K_i$-67, was measured using the ImageJ software (National Institutes of Health).

**2.7. Observation of Scanning Electron Microscope Images for Measuring the Hair Shaft Diameter.** The hair shafts on the back skin were observed under a scanning electron microscope. The back skin, which was prefixed with 2.5% glutaraldehyde for 2 days, was postfixed with 1% osmium tetroxide (Wako, Kyoto, Japan) for 2 h. After dehydration with ethanol, critical point drying was performed (EM CPD300, Leica), followed by gold−palladium coating using an ionic stepper (E101, Hitachi Co., Tokyo, Japan). The samples were observed by using a scanning electron microscope (SEM; JSM-6301F, JEOL, Tokyo, Japan). The diameter of the hair shaft on the skin surface was measured by using ImageJ software.

**2.8. Cell Culture.** HFSCs were isolated from the back skin of mice at 3 weeks, as the methods of Chacón-Martínez et al. and Call et al., with some modifications.[19] The growth medium for HFSCs was used DMEM/F12 (high glucose DMEM without $Ca^{2+}$ or $Mg^{2+}$: Ham's F12 = 3:1, Gibco; Thermo Fisher Scientific) containing 5% fetal bovine serum (Boehringer-Mannheim, Mannheim, Germany), epidermal growth factor (BD Biosciences), fibroblast growth factor-2 (Nacalai, Kyoto, Japan), vascular endothelial growth factor (PeproTech, Rocky Hill, NJ), Y-27632 (MedChemExpress, Monmouth Junction, NJ), ITS-X (Wako), L-glutamine (Wako), bovine pituitary extract (Kurabo, Osaka, Japan), ethanolamine (Sigma-Aldrich), phosphorylethanolamine (Sigma-Aldrich), dexamethasone (Sigma-Aldrich), and 1% penicillin/streptomycin solution (Wako).

The skin on the backs of the mice was removed and washed with D-PBS. The skin was separated into the epidermis and dermis by treatment with 0.8% trypsin for 50 min at 37 °C. Cells obtained by gentle pipetting of the epidermis and dermal surface were passed through a 70-$\mu$m strainer (BD Biosciences). The obtained cells were used as HFSC-containing keratinocytes. The cells were resuspended in the growth medium and seeded in 12-well plates at $0.4 \times 10^5$ cells/well. All cultures were incubated at 37 °C in 5% $CO_2$. One day after seeding, the medium was replaced with growth medium containing 0.01, 0.03, 0.1, and 0.3% RJ and the vehicle (DMEM/F12). HFSC-containing keratinocytes were also cultured with the growth media containing 46 and 138 $\mu$g/mL 10HDAA, 8.5 and 25.5 $\mu$g/mL 10H2DA, 2.8 and 8.4 $\mu$g/mL sebacic acid, and 4.4 and 13 $\mu$g/mL 2-decenedioic acid for reproducing the concentration of each fatty acids in the 0.1 and 0.3% RJ containing growth media.[17] HDAA, 10H2DA, sebacic acid, and 2-decenedioic acid were obtained from Yamada Bee Company, Inc. Two days after cultivation, cells were subjected to immunofluorescence staining and Western blotting.

**2.9. Western Blotting.** Western blotting was performed as previously described.[20] Samples of the cultured cells were lysed in Laemmli SDS-solubilizing buffer and then heated for 15 min at 70 °C. Samples were electrophoresed on sodium dodecyl sulfate-polyacrylamide gels and transferred onto poly(vinylidene difluoride) membranes. After blocking with 4% skim milk, membranes were incubated with primary antibodies diluted in T-PBS containing 2.5% BSA. Horseradish peroxidase-conjugated secondary antibodies and Luminata Forte (Merck Millipore, Darmstadt, Germany) were used to detect the immunoreactive bands. Images of the immunoreactive band were obtained using a Bio-Rad ChemiDo EQ densitometer and Bio-Rad Quantity One software (Bio-Rad Laboratories, Hercules, CA). Relative protein expression levels were measured by a densitometric analysis of the bands. $\beta$-actin was used as an internal control.

**2.10. Cell Proliferation Assays.** The proliferation of human dermal fibroblasts (Takara Bio Inc., Otsu, Japan) was evaluated using WST-8 cell counting kits (Kishida Chemical, Osaka, Japan). Fibroblasts were cultured in high glucose DMEM containing 5% fetal bovine serum at a density of $10^3$/well in 96-well plates for 1 day. Subsequently, fibroblasts were incubated for 1 day with 0.03, 0.1, and 0.3% RJ and the vehicle, followed by 10% WST-8 for 2 h at 37 °C. Absorbance was measured at 450 nm using a microplate reader (iMark, Bio-Rad).

**2.11. Deoxynucleotidyl Transferase dUTP Nick-End Labeling (TUNEL) Assay.** Cell death of HFSCs was detected by using a TUNEL detection kit according to the manufacturer's instructions. In brief, the fixed HFSCs was immersed in terminal deoxynucleotidyl transferase buffer containing deoxynucleotidyl transferase and fluorescein isothiocyanate-labeled dUTP, incubated in a humid atmosphere at 37 °C for 60 min, and subsequently washed with PBS. After staining nuclei with DAPI, fluorescent images were captured using an all-in-one microscope (BZ-X800; KEYENCE, Osaka, Japan).

**2.12. Statistical Analysis.** Data are presented as means ± the standard error of the mean (SEM). Significance values were calculated using the Mann−Whitney U-test for *in vivo* experiments and Student's $t$ test for *in vitro* experiments using EZR software (Saitama Medical Center, Jichi Medical University, Saitama, Japan), a graphical user interface for R (The R Foundation for Statistical Computing, Vienna, Austria). Differences were considered significant at a $p$-value of <0.05. These $p$-values are indicated by *.

## 3. RESULTS

**3.1. Thin Hair Shaft Formation by Topical Application of RJ in the Depilated Mice.** The effects of RJ on hair follicle development were investigated using a forced anagen induction model by depilating the back skin of the mice. Forced depilation synchronized hair cycles throughout the back skin without temporal differences in hair cycle between individuals, as previously reported,[5] in mice treated with


https://doi.org/10.1021/acsomega.4c09123
ACS Omega 2025, 10, 17228−17236

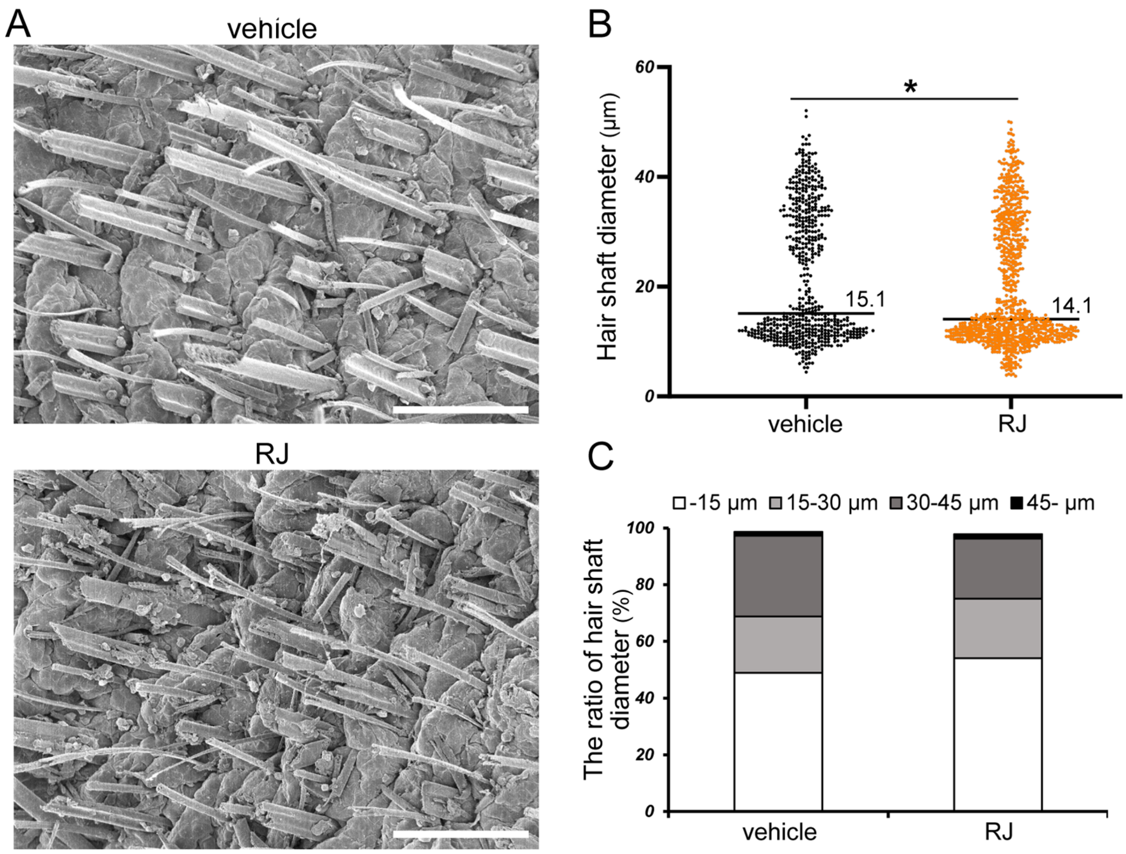


**Figure 1.** Effects of RJ on hair shaft diameter in the forced anagen induction model. (A) Images taken using scanning electron microscopy show the hair shaft on the back skin in the depilated mouse treated with topical applications of RJ or vehicle to depilated back skin for 11 days. Bar = 200 $\mu$m. (B, C) Graphs show the diameter of hair shafts (B) and the ratio of the hair shaft diameter (C). $^*p < 0.05$ ($n$ = 579 of 5 vehicle-treated mice, $n$ = 859 of 7 RJ-treated mice).

vehicle and RJ (Supporting Figure 1A). Detectable differences in proceeding hair cycle were not observed between the mice treated with RJ or with the vehicle. The dermal side of the excised skin was covered with a hair shaft and blacked due to melanin pigment (Supporting Figure 1B), suggesting that the hair cycle of the hair follicles in the back skin was in the late anagen stage. In the sagittal section of the back skin stained with hematoxylin and eosin, well-developed hair follicles in the late anagen phase were observed without any detectable morphological differences between the skin treated with RJ or vehicle (Supporting Figure 1C). The RJ treatment did not affect the structure or thickness of the epidermis (Supporting Figure 1C,D).

To measure the diameter of the hair shaft protruding from the skin, the skin surface was observed with a scanning electron microscope (Figure 1A). The average diameter of the hair shaft on skin treated with RJ was smaller than that on skin treated with the vehicle (Figure 1B). The percentages of the hair shaft diameter at less than 15 $\mu$m were 54 and 49% in skins treated with RJ or with vehicle, respectively (Figure 1C). In contrast, the percentage of the hair shaft diameter at less than 30−45 $\mu$m was 21 and 28% in skins treated with RJ or with vehicle, respectively.

Next, we measured the diameter of the hair bulb in the skin, which was whole-mount immunostained with CK15, a marker of HFSCs, and $K_i$-67, a marker of proliferating cells, with nuclear staining with DAPI.[6] Immunostaining images clearly showed hair bulb structures on the skin (Figure 2A). The average diameter of the hair bulb of skin treated with RJ and vehicle was 73.2 and 75.2 $\mu$m, respectively, without statistical difference (Figure 2B). The percentages of hair bulbs between 80 and 100 $\mu$m in diameter were 20 and 24% in skins treated with RJ or vehicle, respectively (Figure 2C). In contrast, the percentages of hair bulbs between 60 and 80 $\mu$m in diameter were 59 and 53% in skins treated with RJ or with vehicle, respectively, suggesting that RJ tends to increase hair bulbs with smaller diameters.

Immunostaining images of the sagittal section of the hair follicles showed $K_i$-67$^+$ cells in hair bulbs and CK15$^+$ cells in the bulge regions without any detectable morphological changes after RJ treatment compared to those treated with the vehicle (Figure 3A,B). In the bulge regions, CK15$^+$ cells hardly showed $K_i$-67 positive activity in both skins treated with RJ or the vehicle (Figure 3B).

**3.2. RJ Suppresses Proliferation of HFSCs in Developing Hair Follicle in the Shaved Mice.** The hair cycle progressed from the caudal to the cranial end of the back skin in shaved mice.[5] In addition, the late anagen stage is identified by the protrusion of the hair shaft onto the skin surface. After topical application of RJ and vehicle, the hair shaft on the skin surface was observed in the caudal regions of the back skin (Supporting Figure 2A). There was no significant difference in the timing of hair shaft appearance in the caudal regions of the back skin between RJ- and vehicle-treated mice (Supporting Figure 2B). In addition, sagittal sections of skin stained with hematoxylin and eosin showed hair cycle progression from the


https://doi.org/10.1021/acsomega.4c09123
ACS Omega 2025, 10, 17228−17236

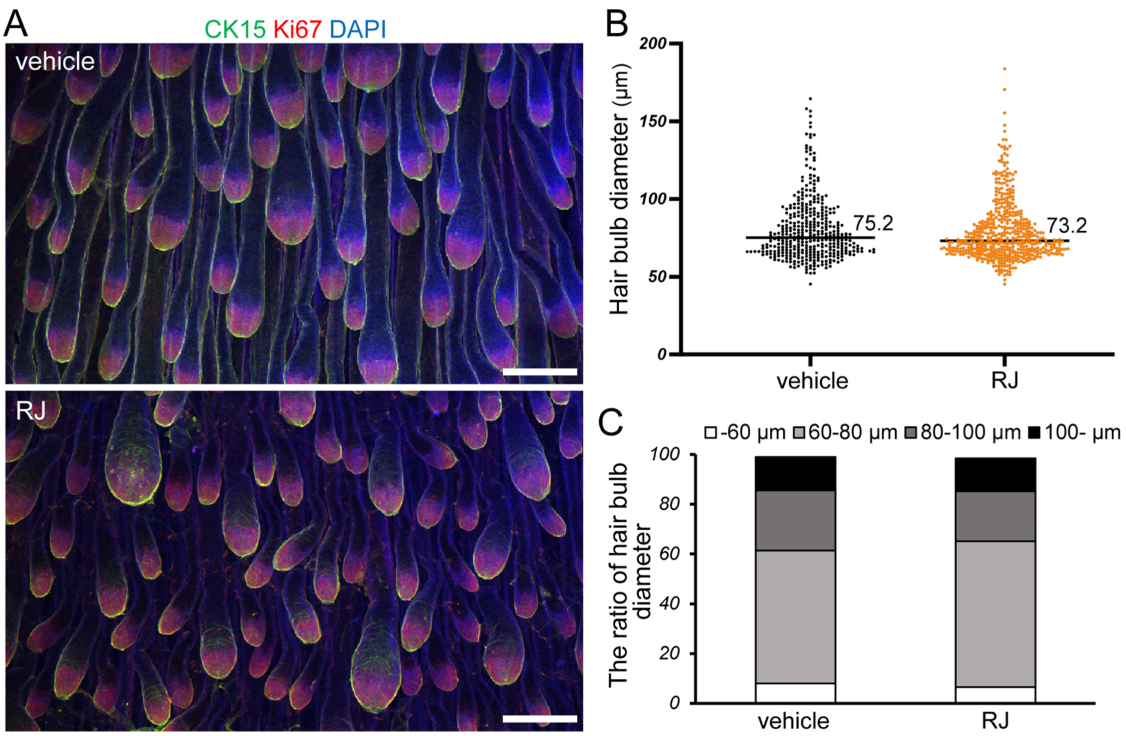


**Figure 2.** Effects of RJ on the diameter of the hair bulb in the forced anagen induction model. (A) Fluorescence images taken using a confocal microscope show the localization of CK15 (green) and $K_i$-67 (red) in the hair bulbs of the back skin treated with topical applications of RJ or vehicle for 11 days. Nuclei were stained with DAPI (blue). Bar = 200 $\mu$m. (B, C) Graphs show the diameter of hair bulbs (B) and the ratio of the hair bulbs diameter (C). $n$ = 389 of 5 vehicle-treated mice, $n$ = 522 of 7 RJ-treated mice.

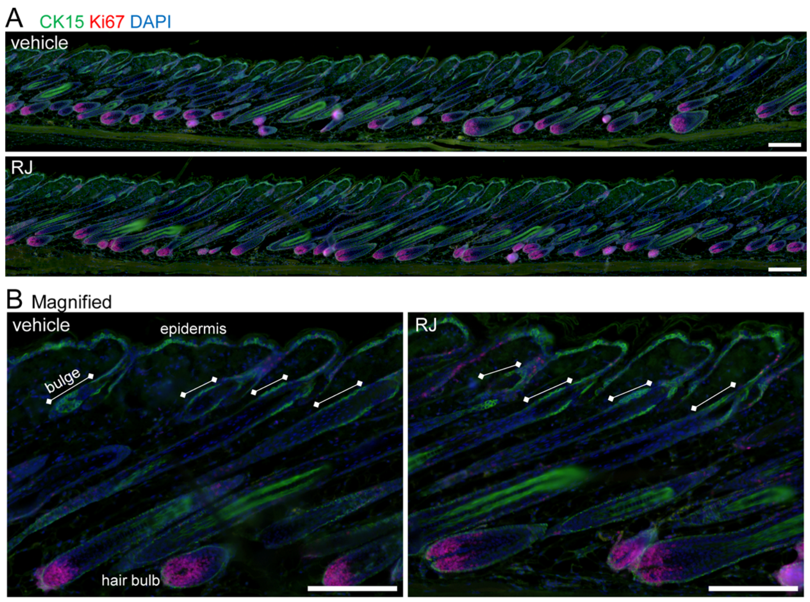


**Figure 3.** Effects of RJ on the proliferation of HFSCs in the hair follicle at the late anagen stage in the forced anagen induction model. (A) Immunostaining images show the localization of CK15 (green) with $K_i$-67 (red) in the sagittal sections of the hair follicle at late anagen stage in the depilated mouse treated with topical applications of RJ or vehicle to the back skins for 11 days. Nuclei were stained with DAPI (blue). Bar = 100 $\mu$m. (B) Magnified images of (A). Bar = 100 $\mu$m.

caudal side toward the cranial side of the back skin, although there were no detectable differences in the hair follicle structures formed between the RJ-treated and vehicle-treated mice (Supporting Figure 2C,D). RJ treatment did not influence epidermal structure or thickness (Supporting Figure 2D,E).

Next, we investigated the influence of RJ on the proliferation of HFSCs in early anagen hair follicles in the shaved back skin using immunostaining for $K_i$-67 and CK15. CK15$^+$ cells were observed in the bulge regions and outer root sheaths below the bulge regions of early anagen hair follicles, as well as in the basal layer of the epidermis (Figure 4A). Some CK15$^+$ cells in the bulge regions and outer root sheaths were $K_i$-67 positive.



https://doi.org/10.1021/acsomega.4c09123
ACS Omega 2025, 10, 17228−17236

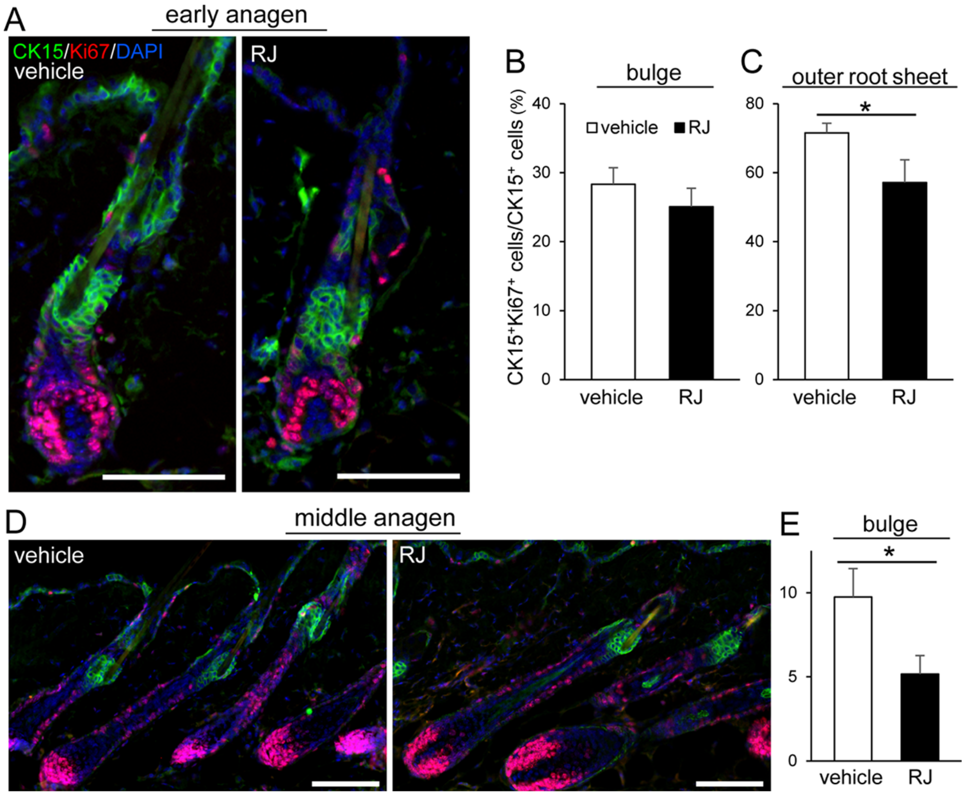


**Figure 4.** Effects of RJ on proliferation of HFSCs in the hair follicle at early and middle anagen stages in the shaved mouse model. (A, B) Immunofluorescence staining images show the localization of CK15 (green) with $K_i$-67 (red) in the sagittal sections of the hair follicle at early (A) and middle (B) anagen stages in the shaved mouse treated with RJ or vehicle to the back skin. Nuclei were stained with DAPI (blue). Bar = 100 $\mu$m. (C−E) Graphs show the ratio of CK15$^+$/$K_i$-67$^+$ cells per CK15$^+$ cells in the bulge regions (C, E) and the regions between the bulge and the hair bulb (D). $n$ = 21 of 5 vehicle-treated mice and 15 of 5 RJ-treated mice.

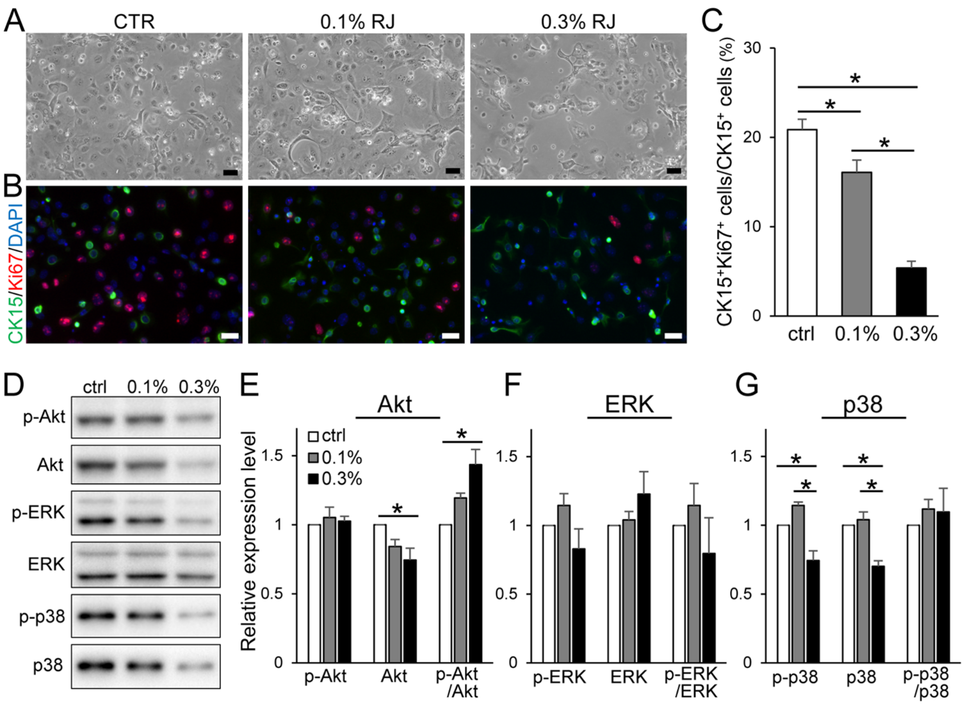


**Figure 5.** Effects of RJ on proliferation of HFSCs *in vitro*. (A) Keratinocytes and HFSCs isolated from the mouse back skins were cultured with 0.1 and 0.3% RJ containing medium for 2 days. (B) Cultured cells were immunostained with $K_i$-67 and CK15. (C) Graphs show the ratio of CK15$^+$/$K_i$-67$^+$ cells per CK15$^+$ cells in the cultured cell layers. Bar = 50 $\mu$m. (D−G) Results of Western blotting (D) and densitometry analyses of Akt and phosphorylated Akt (pAkt; E), ERK and pERK (F), and p38 and pp38 (G). DNA concentration in SDS-PAGE samples was used as an internal control. The data are presented as the mean ± SEM; $n$ = 6. Asterisks indicate the significant differences ($p < 0.05$).


https://doi.org/10.1021/acsomega.4c09123
*ACS Omega* 2025, 10, 17228−17236

There was no significant difference in the ratio of CK15$^+$ cells to $K_i$-67$^+$ cells in the bulge regions between the skins treated with vehicle and RJ (Figure 4B). In the outer root sheaths below the bulge regions, the ratio of CK15$^+$ cells to Ki67$^+$ cells in skin treated with RJ was significantly lower than that in skin treated with vehicle (Figure 4C). In addition, the bulge regions of the middle anagen phase showed a lower ratio of CK15$^+$ cells per $K_i$-67$^+$ cells in the skin treated with RJ than in those treated with vehicle (Figure 4D,E).

**3.3. RJ Suppresses Proliferation of CK15$^+$ Cells and Modulates Activation State of Akt and MAPK Signaling.** The effect of RJ on CK15$^+$ cell proliferation was examined by culturing skin epithelial cells, including HFSCs and progenitor cells, which are CK15 positive. Untreated cells and those treated with 0.1% RJ for 2 days exhibited a cobblestone-like shape, whereas 0.3% RJ treatment induced contraction shrinkage in some cells (Figure 5A). Immunostaining images showed that parts of the untreated and 0.1% RJ were $K_i$-67 and CK15 positive (Figure 5B). However, there were fewer $K_i$-67$^+$and CK15$^+$ cells in the RJ-treated cells. The ratios of $K_i$-67$^+$ to CK15$^+$ cells in untreated, 0.1% RJ, and 0.3% RJ were 21, 16, and 5%, respectively (Figure 5C).

Subsequently, the influence of RJ on the activation of Akt, ERK, and p38 by examining their phosphorylation and total expression levels were investigated using Western blotting. Samples were standardized according to the amount of DNA. The relative expression levels of total Akt were reduced in cells treated with 0.1 and 0.3% RJ for 2 days compared to those in untreated cells, whereas the phosphorylation rate of Akt was increased by RJ treatment in a dose-dependent manner (Figure 5D,E). There was no significant effect on pERK or total ERK RJ treatment (Figure 5F). The relative expression levels of pp38 were reduced by 0.3% RJ treatment compared to those in untreated cells and cells treated with 0.1% RJ, whereas 0.1% RJ treatment increased the relative expression levels of phosphorylated and total p38 (Figure 5G). We further investigated the effect of lower concentrations of RJ on HFSCs because 0.1% RJ suppressed the proliferation of CK15$^+$ cells and induced the activation of p38. The results showed the phosphorylation rate of p38 was increased by 0.03% RJ treatment whereas there had no significant effect on the ratio of $K_i$-67$^+$ to CK15$^+$ cells and the phosphorylation rate of Akt and ERK (Supporting Figure 3).

RJ contains 10HDAA, 10H2DA, sebacic acid, and 2-decenedioic acid as active ingredients to regulate cell behavior.[2] Finally, we investigated whether four types of fatty acids at the equivalent concentrations found in the 0.1 or 0.3% RJ influence $K_i$-67$^+$/CK15$^+$ cells, Akt and p38. However, the detectable differences were not observed in the $K_i$-67$^+$/CK15$^+$ cells treated with each type of fatty acids compared to those in control (Supporting Figure 4). In addition, four kinds of fatty acids were hardly influenced in phosphorylation rate of Akt and p38 (Supporting Figure 5).

## 4. DISCUSSION

RJ is a honeybee product to facilitate cutaneous wound healing by stimulating keratinocyte proliferation.[4] Hair follicles are skin appendages that form hair shafts. Both hair follicles and hair shafts consist of keratinocytes differentiated from HFSCs. However, it remains unclear whether RJ influences hair follicle development and shaft formation. In this study, we investigated the effects of RJ on hair shaft formation by topical application of RJ on depilated mouse back skin, in which the hair cycle of all hair follicles was synchronized.[5] The results showed that topical application of RJ induced thinning of the hair shaft concurrently with a change in the ratio of the hair bulb diameter. In shaved mouse back skin, the topical application of RJ suppressed the proliferation of CK15$^+$ cells in hair follicles at the early and middle anagen stages without influencing the hair cycle. HFSCs in bulge regions and secondary hair germs actively proliferate after the initiation of anagen, and progenitor cells originating from HFSCs form the lower parts of the hair follicle containing hair bulbs, in which the hair shaft is formed.[21] RJ suppresses the proliferation of cultured CK15$^+$ cells *in vitro* CK15 is a marker of HFSCs and progenitor cells.[6] These findings suggest that RJ suppresses hair follicle maturation around the middle anagen phase by affecting the proliferation of HFSCs and progenitor cells, resulting in the formation of thin hair shafts.

In this study, topical application of RJ suppressed the proliferation of HFSCs and progenitor cells in the development of hair follicles. RJ also inhibited the proliferation of CK15$^+$ cells concurrently with Akt and p38 activation *in vitro*. Akt are signaling molecules regulates cell proliferation, survival, and metabolism whereas p38 regulates inflammation and cell death.[22,23] Akt is activated in the bulge region and hair bulb during drug-induced hair regeneration concurrently with the active proliferation of HFSCs.[24] Previous studies have shown that RJ modulates the activation of p38 and Akt.[9,25] In preliminary experiments to verify the biocompatibility of RJ, RJ did not influence proliferation of dermal fibroblasts and cell death of HFSCs (Supporting Figure 6). Furthermore, topical application of RJ did not cause inflammation detected as activation of NF$\kappa$B and migration of neutrophils in mouse back skins (Supporting Figure 7). These findings suggest that p38 and Akt signaling pathways are involved in the suppressive effects of RJ on the proliferation of HFSCs and progenitor cells.

The main components of RJ are water, sugars, proteins, and fatty acids. The protein and fatty acid components of RJ exhibit various physiological activities.[26] The major royal jelly proteins royalisin and apismin are RJ-specific proteins. RJ contains 10HDAA, 10H2DA, sebacic acid, and 2-decenedioic acid as fatty acid components.[2] In this study, protease-treated RJ, which degrades RJ proteins to peptides and amino acids using proteases, was used to reduce immunoreactivity and allergenicity.[16] In addition, protease-treated RJ contains 4.3% 10H2DA, 1.3% 10HDAA, 0.3% sebacic acid, and 0.4% 2-decenedioic acid as major fatty acid components in addition to minerals and vitamins.[19] Hydrophilic substances with a molecular weight of more than 500 Da, such as proteins and polypeptides, hardly cross the epidermal barrier of the stratum corneum or the tight junctions of the granular layer.[27] HFSCs reside inside epithelial tight junctions in hair follicles.[28] These findings suggest that the protein components of RJs cannot react with HFSCs in developing hair follicles *in vivo*. By contrast, fatty acids in addition to hydrophilic substances with a molecular weight of more than 500 Da such as minerals and vitamins pass through the epidermal barrier.[29] Previous studies have reported that fatty acid components of RJ enhance proliferation of mammary epithelial cell lines and modulate dendritic cell-mediated immune response.[2,30] In addition, 10-HDA of royal jelly acid induced p38 activation and ERK inactivation in human lung cancer cells,[31] similar to the RJ treatment of skin epithelial cells in this study. Therefore, it was hypothesized that fatty acids (10H2DA, 10HDAA, sebacic


https://doi.org/10.1021/acsomega.4c09123
ACS Omega 2025, 10, 17228−17236

acid, and 2-decenedioic acid) regulate HFSCs and investigated the influences of them in *in vitro* experiments using HFSCs. However, at concentrations equivalent to 0.1 and 0.3% RJ, these fatty acids had no effect on follicular stem cell proliferation or signaling pathways of Akt and p38. These findings suggest that the effect of RJ on HFSCs cannot be attributed to at least a single fatty acid. Minor ingredients other than these fatty acids or the combination of multiple fatty acids may inhibit hair follicle development and HFSCs proliferation.

In this study, we demonstrated the suppressive effects of RJ on hair follicle development in the early mid anagen phase and thin hair shaft formation in the late anagen phase. RJ also suppresses the proliferation of HFSCs and progenitor cells in the development of hair follicles. Furthermore, RJ suppressed the proliferation of HFSCs and progenitor cells concurrently with the inactivation of Akt and activation of p38 *in vitro*. These findings suggest that RJ suppresses hair follicle development by regulating the HFSC proliferation of HFSCs regulated by Akt and p38 signaling. Such functions of RJ may contribute to the treatment of hypertrichosis. In addition, it may help suppress excess hair growth in unwanted hair areas as a cosmetic ingredient. Further investigation is required to determine how to best apply RJ to human skin and the active components in RJs by *in vitro* skin permeation testing using human skin fragments and/or the reconstructed skins.

## ■ ASSOCIATED CONTENT

### Supporting Information

The Supporting Information is available free of charge at https://pubs.acs.org/doi/10.1021/acsomega.4c09123.

> Additional experimental data including effects of RJ on hair growth; activation of NFκB; and migration of neutrophils in the forced anagen induction model; effects of RJ on hair cycle and hair follicle development in the shaved mouse model; effects of RJ at lower concentrations on proliferation of HFSCs *in vitro*; effects of fatty acids contained in RJ on HFSCs and their Akt and MAPK signaling *in vitro*; and effects of RJ on proliferation of dermal fibroblasts and cell death of HFSCs *in vitro* (PDF)

## ■ AUTHOR INFORMATION


### Corresponding Author

**Ken Kobayashi** − *Laboratory of Cell and Tissue Biology, Research Faculty of Agriculture, Hokkaido University, 060-8589 Sapporo, Japan;* orcid.org/0000-0002-2846-6887; Phone: +81-11-706-2540; Email: kkobaya@agr.hokudai.ac.jp

### Authors

**Takumi Hamanishi** − *Laboratory of Cell and Tissue Biology, Research Faculty of Agriculture, Hokkaido University, 060-8589 Sapporo, Japan*

**Haruta Koga** − *Laboratory of Cell and Tissue Biology, Research Faculty of Agriculture, Hokkaido University, 060-8589 Sapporo, Japan*

**Takanori Nishimura** − *Laboratory of Cell and Tissue Biology, Research Faculty of Agriculture, Hokkaido University, 060-8589 Sapporo, Japan*

Complete contact information is available at: https://pubs.acs.org/10.1021/acsomega.4c09123


### Notes

The authors declare the following competing financial interest(s): K.K. was supported by a Yamada Research Grant and provided protease-treated royal jelly from Yamada Bee Company, Inc.

## ■ ACKNOWLEDGMENTS

We are grateful to Maho Miyashita, Laboratory of Dairy Food Science, Research, Faculty of Agriculture, Hokkaido University, for helpful advice.

## ■ ABBREVIATIONS

BSA, bovine serum albumin; D-PBS, Dulbecco's-PBS; HFSC, hair follicle stem cells; 10HDAA, 10-hydroxydecanoic acid; 10H2DA, 10-hydroxy-trans-2-decenoic acid; pAkt, phosphorylated-Akt; RJ, royal jelly; SEM, standard error of the mean; T-PBS, PBS containing 0.05% Tween-20

## ■ REFERENCES


(1) Fratini, F.; Cilia, G.; Mancini, S.; Felicioli, A. Royal Jelly: An ancient remedy with remarkable antibacterial properties. *Microbiol. Res.* **2016**, *192*, 130−141.

(2) Vucevic, D.; Melliou, E.; Vasilijic, S.; Gasic, S.; Ivanovski, P.; Chinou, I.; Colic, M. Fatty acids isolated from royal jelly modulate dendritic cell-mediated immune response in vitro. *Int. Immunopharmacol.* **2007**, *7* (9), 1211−1220.

(3) (a) Pasupuleti, V. R.; Sammugam, L.; Ramesh, N.; Gan, S. H. Honey, Propolis, and Royal Jelly: A Comprehensive Review of Their Biological Actions and Health Benefits. *Oxid. Med. Cell. Longevity* **2017**, *2017*, No. 1259510. (b) Khazaei, M.; Ansarian, A.; Ghanbari, E. New Findings on Biological Actions and Clinical Applications of Royal Jelly: A Review. *J. Diet. Suppl.* **2018**, *15* (5), 757−775.

(4) (a) Lin, Y.; Zhang, M.; Wang, L.; Lin, T.; Wang, G.; Peng, J.; Su, S. The in vitro and in vivo wound-healing effects of royal jelly derived from Apis mellifera L. during blossom seasons of Castanea mollissima Bl. and Brassica napus L. in South China exhibited distinct patterns. *BMC Complementary Med. Ther.* **2020**, *20* (1), No. 357. (b) Lin, Y.; Zhang, M.; Lin, T.; Wang, L.; Wang, G.; Chen, T.; Su, S. Royal jelly from different floral sources possesses distinct wound-healing mechanisms and ingredient profiles. *Food Funct.* **2021**, *12* (23), 12059−12076.

(5) Müller-Röver, S.; Foitzik, K.; Paus, R.; Handjiski, B.; van der Veen, C.; Eichmuller, S.; McKay, I. A.; Stenn, K. S. A comprehensive guide for the accurate classification of murine hair follicles in distinct hair cycle stages. *J. Invest. Dermatol.* **2001**, *117* (1), 3−15.

(6) Lyle, S.; Christofidou-Solomidou, M.; Liu, Y.; Elder, D. E.; Albelda, S.; Cotsarelis, G. Human hair follicle bulge cells are biochemically distinct and possess an epithelial stem cell phenotype. *J. Invest. Dermatol. Symp. Proc.* **1999**, *4* (3), 296−301.

(7) Panteleyev, A. A. Functional anatomy of the hair follicle: The Secondary Hair Germ. *Exp. Dermatol.* **2018**, *27* (7), 701−720.

(8) (a) Kamiya, T.; Watanabe, M.; Hara, H.; Mitsugi, Y.; Yamaguchi, E.; Itoh, A.; Adachi, T. Induction of Human-Lung-Cancer-A549-Cell Apoptosis by 4-Hydroperoxy-2-decenoic Acid Ethyl Ester through Intracellular ROS Accumulation and the Induction of Proapoptotic CHOP Expression. *J. Agric. Food Chem.* **2018**, *66* (41), 10741−10747. (b) Pandeya, P. R.; Lamichhane, R.; Lee, K. H.; Kim, S. G.; Lee, D. H.; Lee, H. K.; Jung, H. J. Bioassay-guided isolation of active anti-adipogenic compound from royal jelly and the study of possible mechanisms. *BMC Complement. Altern. Med.* **2019**, *19* (1), No. 33. (c) You, M.; Miao, Z.; Pan, Y.; Hu, F. Trans-10-hydroxy-2-decenoic acid alleviates LPS-induced blood-brain barrier dysfunction by activating the AMPK/PI3K/AKT pathway. *Eur. J. Pharmacol.* **2019**, *865*, No. 172736. (d) Takahashi, K.; Sugiyama, T.; Tokoro, S.; Neri, P.; Mori, H. Inhibitory effect of 10-hydroxydecanoic acid on lipopolysaccharide-induced nitric oxide production via translational downregulation of interferon regulatory factor-1 in RAW264 murine

macrophages. *Biomed. Res.* **2013**, *34* (4), 205−214. (e) Yang, X. Y.; Yang, D. S.; Wei, Z.; Wang, J. M.; Li, C. Y.; Hui, Y.; Lei, K. F.; Chen, X. F.; Shen, N. H.; Jin, L. Q.; et al. 10-Hydroxy-2-decenoic acid from Royal jelly: a potential medicine for RA. *J. Ethnopharmacol.* **2010**, *128* (2), 314−321.

(9) Chi, X.; Liu, Z.; Wei, W.; Hu, X.; Wang, Y.; Wang, H.; Xu, B. Selenium-rich royal jelly inhibits hepatocellular carcinoma through PI3K/AKT and VEGF pathways in H22 tumor-bearing mice. *Food Funct.* **2021**, *12* (19), 9111−9127.

(10) Sugawara, K.; Zakany, N.; Tiede, S.; Purba, T.; Harries, M.; Tsuruta, D.; Biro, T.; Paus, R. Human epithelial stem cell survival within their niche requires ″tonic″ cannabinoid receptor 1-signalling-Lessons from the hair follicle. *Exp. Dermatol.* **2021**, *30* (4), 479−493.

(11) (a) Niu, H.; Li, H.; Guan, Y.; Zhou, X.; Li, Z.; Zhao, S. L.; Chen, P.; Tan, T.; Zhu, H.; Bergdall, V.; et al. Sustained delivery of rhMG53 promotes diabetic wound healing and hair follicle development. *Bioact. Mater.* **2022**, *18*, 104−115. (b) Lu, Q.; Gao, Y.; Fan, Z.; Xiao, X.; Chen, Y.; Si, Y.; Kong, D.; Wang, S.; Liao, M.; Chen, X.; et al. Amphiregulin promotes hair regeneration of skin-derived precursors via the PI3K and MAPK pathways. *Cell Prolif.* **2021**, *54* (9), No. e13106.

(12) (a) Chen, Y.; Fan, Z.; Wang, X.; Mo, M.; Zeng, S. B.; Xu, R. H.; Wang, X.; Wu, Y. PI3K/Akt signaling pathway is essential for de novo hair follicle regeneration. *Stem Cell Res. Ther.* **2020**, *11* (1), No. 144. (b) Sunkara, R. R.; Mehta, D.; Sarate, R. M.; Waghmare, S. K. BMP-AKT-GSK3beta Signaling Restores Hair Follicle Stem Cells Decrease Associated with Loss of Sfrp1. *Stem Cells* **2022**, *40* (9), 802−817.

(13) Kim, J. Y.; Ohn, J.; Yoon, J. S.; Kang, B. M.; Park, M.; Kim, S.; Lee, W.; Hwang, S.; Kim, J. I.; Kim, K. H.; Kwon, O. Priming mobilization of hair follicle stem cells triggers permanent loss of regeneration after alkylating chemotherapy. *Nat. Commun.* **2019**, *10* (1), No. 3694.

(14) Miyata, S.; Oda, Y.; Matsuo, C.; Kumura, H.; Kobayashi, K. Stimulatory effect of Brazilian propolis on hair growth through proliferation of keratinocytes in mice. *J. Agric. Food Chem.* **2014**, *62* (49), 11854−11861.

(15) Ishimatsu-Tsuji, Y.; Moro, O.; Kishimoto, J. Expression profiling and cellular localization of genes associated with the hair cycle induced by wax depilation. *J. Invest. Dermatol.* **2005**, *125* (3), 410−420.

(16) Moriyama, T.; Yanagihara, M.; Yano, E.; Kimura, G.; Seishima, M.; Tani, H.; Kanno, T.; Nakamura-Hirota, T.; Hashimoto, K.; Tatefuji, T.; et al. Hypoallergenicity and immunological characterization of enzyme-treated royal jelly from Apis mellifera. *Biosci., Biotechnol., Biochem.* **2013**, *77* (4), 789−795.

(17) Yamaga, M.; Imada, T.; Tani, H.; Nakamura, S.; Yamaki, A.; Tsubota, K. Acetylcholine and Royal Jelly Fatty Acid Combinations as Potential Dry Eye Treatment Components in Mice. *Nutrients* **2021**, *13* (8), No. 2536.

(18) Yamamoto, K.; Yamauchi, M. Characterization of dermal type I collagen of C3H mouse at different stages of the hair cycle. *Br. J. Dermatol.* **1999**, *141* (4), 667−675.

(19) (a) Chacón-Martínez, C. A.; Klose, M.; Niemann, C.; Glauche, I.; Wickstrom, S. A. Hair follicle stem cell cultures reveal self-organizing plasticity of stem cells and their progeny. *EMBO J.* **2017**, *36* (2), 151−164. (b) Call, M.; Meyer, E. A.; Kao, W. W.; Kruse, F. E.; Schlotzer-Schrehardt, U. Hair Follicle Stem Cell Isolation and Expansion. *Bio. Protoc.* **2018**, *8* (10), No. e2848, DOI: 10.21769/BioProtoc.2848.

(20) Kobayashi, K.; Han, L.; Koyama, T.; Lu, S. N.; Nishimura, T. Sweet taste receptor subunit T1R3 regulates casein secretion and phosphorylation of STAT5 in mammary epithelial cells. *Biochim. Biophys. Acta, Mol. Cell Res.* **2023**, *1870* (4), No. 119448.

(21) Lyle, S.; Christofidou-Solomidou, M.; Liu, Y.; Elder, D. E.; Albelda, S.; Cotsarelis, G. The C8/144B monoclonal antibody recognizes cytokeratin 15 and defines the location of human hair follicle stem cells. *J. Cell Sci.* **1998**, *111* (Pt 21), 3179−3188.

(22) Hers, I.; Vincent, E. E.; Tavare, J. M. Akt signalling in health and disease. *Cell Signalling* **2011**, *23* (10), 1515−1527.

(23) Xia, Z.; Dickens, M.; Raingeaud, J.; Davis, R. J.; Greenberg, M. E. Opposing effects of ERK and JNK-p38 MAP kinases on apoptosis. *Science* **1995**, *270* (5240), 1326−1331.

(24) Qiu, W.; Lei, M.; Zhou, L.; Bai, X.; Lai, X.; Yu, Y.; Yang, T.; Lian, X. Hair follicle stem cell proliferation, Akt and Wnt signaling activation in TPA-induced hair regeneration. *Histochem. Cell Biol.* **2017**, *147* (6), 749−758.

(25) You, M. M.; Chen, Y. F.; Pan, Y. M.; Liu, Y. C.; Tu, J.; Wang, K.; Hu, F. L. Royal Jelly Attenuates LPS-Induced Inflammation in BV-2 Microglial Cells through Modulating NF-kappaB and p38/JNK Signaling Pathways. *Mediators Inflammation* **2018**, *2018*, No. 7834381.

(26) Guo, J. Y.; Wang, Z. X.; Chen, Y. X.; Cao, J.; Tian, W. L.; Ma, B. C.; Dong, Y. L. Active components and biological functions of royal jelly. *J. Funct. Foods* **2021**, *82*, No. 104514.

(27) Andrews, S. N.; Jeong, E.; Prausnitz, M. R. Transdermal delivery of molecules is limited by full epidermis, not just stratum corneum. *Pharm. Res.* **2013**, *30* (4), 1099−1109.

(28) Lay, K.; Yuan, S.; Gur-Cohen, S.; Miao, Y.; Han, T.; Naik, S.; Pasolli, H. A.; Larsen, S. B.; Fuchs, E. Stem cells repurpose proliferation to contain a breach in their niche barrier. *eLife* **2018**, *7*, No. e41661, DOI: 10.7554/eLife.41661.

(29) Mittal, A.; Sara, U. V.; Ali, A.; Aqil, M. Status of fatty acids as skin penetration enhancers-a review. *Curr. Drug Delivery* **2009**, *6* (3), 274−279.

(30) Suzuki, K. M.; Isohama, Y.; Maruyama, H.; Yamada, Y.; Narita, Y.; Ohta, S.; Araki, Y.; Miyata, T.; Mishima, S. Estrogenic activities of Fatty acids and a sterol isolated from royal jelly. *Evidence Based Complementary Altern. Med.* **2008**, *5* (3), 295−302.

(31) Lin, X. M.; Liu, S. B.; Luo, Y. H.; Xu, W. T.; Zhang, Y.; Zhang, T.; Xue, H.; Zuo, W. B.; Li, Y. N.; Lu, B. X.; et al. 10-HDA Induces ROS-Mediated Apoptosis in A549 Human Lung Cancer Cells by Regulating the MAPK, STAT3, NF-kappaB, and TGF-beta1 Signaling Pathways. *BioMed Res. Int.* **2020**, *2020*, No. 3042636.


https://doi.org/10.1021/acsomega.4c09123
ACS Omega 2025, 10, 17228−17236